

Low-frequency finite-element modelling of the gerbil middle ear

Nidal Elkhouri¹, Hengjin Liu¹ and W. Robert J. Funnell^{1,2}

¹Dept. BioMedical Engineering, McGill University, Montréal, QC, Canada H3B 2B4

²Dept. Otolaryngology, McGill University, Montréal, QC, Canada H3B 2B4

Corresponding author:

W.R.J. Funnell

Dept. BioMedical Engineering

McGill University

3775, rue University

Montréal, QC H3A 2B4

Canada

Tel: +1-514-398-6739

Fax: +1-514-398-7461

E-mail: robert.funnell@mcgill.ca

ABSTRACT

The gerbil is a popular species for experimental middle-ear research. The goal of this study is to develop a 3-D finite-element model to quantify the mechanics of the gerbil middle ear at low frequencies (up to about 1 kHz). The 3-D reconstruction is based on a magnetic-resonance-imaging dataset with a voxel size of about 45 μm , and an X-ray micro-CT dataset with a voxel size of about 5.5 μm , supplemented by histological images. The eardrum model is based on moiré shape measurements. Each individual structure in the model was assumed to be homogeneous with isotropic, linear and elastic material properties derived from *a priori* estimates in the literature.

The behaviour of the finite-element model in response to a uniform acoustic pressure on the eardrum of 1 Pa is analyzed. Sensitivity tests are done to evaluate the significance of the various parameters in the finite-element model. The Young's modulus and the thickness of the pars tensa have the most significant effect on the load transfer between the eardrum and the ossicles and, along with the Young's modulus of the pedicle and stapedial annular ligament, on the displacements of the stapes.

Overall, the model demonstrates good agreement with low-frequency experimental data. For example, (1) the maximum footplate displacement is about 35 nm; (2) the umbo/stapes displacement ratio is found to be about 3.5; (3) the motion of the stapes is predominantly piston-like; and (4) the displacement pattern of the eardrum shows two points of maximum displacement, one in the posterior region and one in the anterior region. The effects of removing or stiffening the ligaments are comparable to those observed experimentally.

Keywords: middle ear, gerbil, pedicle, low-frequency, finite-element model, mechanics.

I. INTRODUCTION

The middle ear is the site of many infections and birth defects, among other problems. Middle-ear prostheses and non-invasive diagnostic tools are often unsatisfactory. In attempts to improve our understanding of middle-ear mechanics, many groups have conducted experimental work on mammalian middle ears. In particular, gerbils are becoming popular for middle-ear research, in part because they are inexpensive and their middle-ear structures are easily accessible.

Mathematical models are useful for helping with the interpretation of experimental data and for providing additional insight. Lumped-parameter models were the first ones used to study the middle ear. Although these models are able to replicate some experimental data, their parameters are not closely tied to anatomical or physiological data. Nowadays, finite-element models are commonly used in middle-ear research. They are based on anatomical shapes, biological material properties, and realistic boundary conditions and loading conditions. The application of such models to middle-ear research was introduced by Funnell & Laszlo (1978).

A number of authors have since used the finite-element method to study the mechanics of the eardrum and ossicles in humans (Wada *et al.*, 1992; Beer *et al.*, 1999; Bornitz *et al.*, 1999; Prendergast *et al.*, 1999; Koike *et al.*, 2002; Sun *et al.*, 2002) and in cats (Funnell & Laszlo, 1978; Funnell *et al.*, 1987; Ladak & Funnell, 1996; Funnell *et al.*, 2005). The geometries have generally been oversimplified and material properties have often been based on curve fitting. Although a number of experimental studies have been conducted on gerbil middle ears (von Unge *et al.*, 1993; Rosowski *et al.*, 1999, Olson & Cooper, 2000; Dirckx & Decraemer, 2001; Overstreet *et al.*, 2003; Ravicz & Rosowski, 2004), the only finite-element model for the gerbil was a preliminary one presented by

Funnell *et al.* (1999, 2000). The aim of this study is to present a detailed finite-element model of the gerbil middle ear and to quantify its mechanics at low frequencies based on *a priori* material-property estimates from the literature. No attempt was made to match experimental measurements by adjusting model parameters. The geometry was defined accurately with the use of magnetic-resonance imaging and X-ray micro-CT data, supplemented by histological images, and of moiré topography. Sensitivity tests were performed to evaluate the significance of certain parameters in the finite-element model. The behaviour of the model was compared with previous experimental measurements on gerbil middle ears.

II. FINITE-ELEMENT MODEL

A. Geometry and material properties

As in our previous gerbil model (Funnell *et al.*, 1999, 2000), the ossicles were generated from magnetic resonance microscopy (MRM) images with a voxel size of about 45 μm , and the eardrum was based on images from phase-shift moiré topography. Because of its extremely small thickness, the stapes annular ligament in this new model

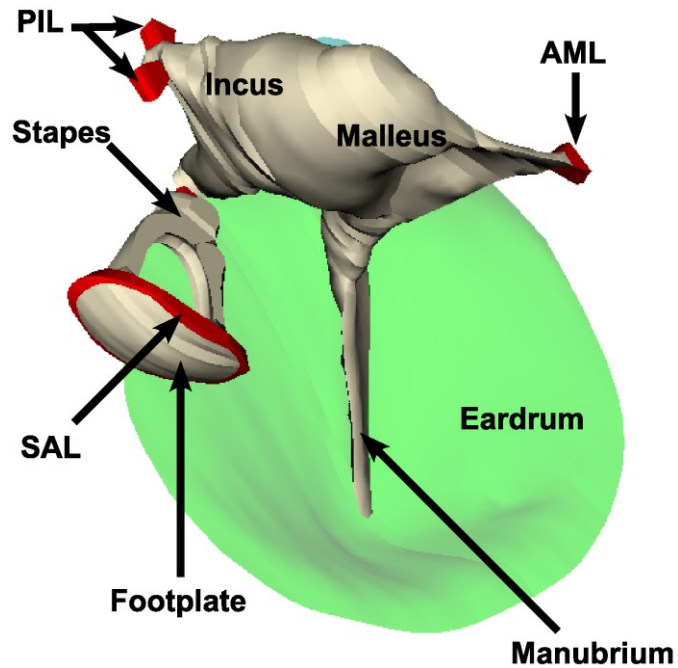


Figure 1: Complete gerbil middle-ear model. AML: anterior malleal ligament; PIL: posterior incudal ligament; SAL: stapes annular ligament.

was based on X-ray micro-CT images with a voxel size of about 5.5 μm . Histological serial sections were used to supplement the MRM and micro-CT images. For example, histology was very helpful in defining the exact points of origin and insertion of the ligaments and their shapes.

The model simulates the behaviour of the gerbil middle ear in response to uniform sound pressures of low enough frequencies that inertial and damping effects may be neglected. At these frequencies the middle-ear system is stiffness-dominated. Fig. 1 shows the new model. For simplicity, each individual structure of the model was assumed to be homogeneous with isotropic, linear and elastic properties. Isotropy is used as an initial approximation because there is no strong direct evidence of anisotropy in the middle-ear structures. The structures of the model are the eardrum, the malleus, the incus, the stapes, the anterior malleolar ligament, the posterior incudal ligament, and the stapedia annular ligament. The mechanical properties of each structure are described in the following sections.

In the absence of experimental measurements, the Poisson's ratio was assumed to be 0.3. Although 0.3 is a reasonable value for bone, it might be argued that Poisson's ratio should be close to 0.5 for soft tissues, since they are thought to be nearly incompressible. Values near 0.5, however, cause numerical problems for the finite-element formulation used here. Increasing Poisson's ratio to 0.4 for the soft tissues in this model produced displacement changes of less than 10%, consistent with previous modelling (e.g., Qi *et al.*, 2004). This is also consistent with the theoretical relationship $G = E/2(1+\nu)$ between Poisson's ratio (ν), Young's modulus (E) and the shear modulus (G), and the assumption that the annular ligament operates primarily in shear (Lynch *et al.*, 1982). This relationship predicts that the effect of increasing Poisson's ratio to 0.5

would be only about 15% for the annular ligament. The effects for the eardrum, malleal ligament and incudal ligament would be expected to be smaller because their configurations do not lead to major constraints on volume changes.

1. Eardrum

The eardrum is represented by 1101 triangular thin-shell elements. These elements include both bending and membrane (in-plane) stiffnesses. The geometry of the eardrum is based on phase-shift moiré topography, a non-contacting optical method that can measure the precise 3-D shape of an object (Dirckx & Decraemer, 1989, 1990). The Young's modulus of the pars tensa (PT) was set to 60 MPa, based on a recent study by Fay *et al.* (2005), who used theoretical methods to assess Young's modulus values for cat and human eardrums. For an isotropic cat model, Fay *et al.* estimated ranges for the Young's modulus of 30–60 MPa for the posterior region of the PT and 60–90 MPa for the anterior region, so the value of 60 MPa is consistent with our assumption of uniformity. The overall microstructure of the gerbil PT is similar to that of the human and cat PT, and therefore 60 MPa seems to be a reasonable estimate for the present model.

Given the lack of measurements on the mechanical properties of the pars flaccida (PF), Koike *et al.* (2002) assumed that the Young's modulus of the PF is one third of that of the PT. Using the same ratio, we set the Young's modulus of the PF to 20 MPa. The PT and the PF were assigned uniform thicknesses of 7 μm and 24 μm , respectively, based on measurements by Kuypers *et al.* (2005).

The outer ends of the eardrum – where it meets the fibrocartilaginous ring – were fully clamped. In a finite-element model analysis of the moustached bat, Van Wijhe *et al.* (2000) simulated forces applied to the fibrocartilaginous ring and observed that the ring

was much more rigid than the eardrum, at least at low frequencies.

2. Ossicles

To simplify the model and speed up the simulations, we modelled the ossicles as hollow shells composed of triangular surface elements, rather than as solid bodies filled with volume elements. For a given amount of surface detail, the representation as hollow shells greatly reduces the number of degrees of freedom in the finite-element solution by avoiding internal nodes. This is acceptable since the ossicles are assumed to behave like rigid structures, at least at low frequencies (Guinan & Peake, 1967; Gundersen *et al.*, 1976), and since the mass distribution does not matter at frequencies low enough that inertial effects are negligible. The ossicles were represented with 4717 triangular shell elements.

The thicknesses of the shell elements for the ossicles were adapted to their geometries, based on direct measurements from the MRM images. In a slice that best showed the average shape of the solid structure, the approximate diameter was measured, and elements for that structure were given a thickness equal to about one third of the diameter of the structure. In regions within a structure where the thickness changed considerably, different thicknesses were assigned. Thicknesses of 156 μm , 63 μm and 10 μm were assigned to the malleus head, neck and manubrium, respectively. The thicknesses assigned to the incus were 156 μm for the head, 50 μm for the long process, 21 μm for the lenticular plate, and 36 μm for the posterior process. The thicknesses assigned to the stapes were 42 μm for the head, 21 μm for both crura, and 31 μm for the footplate.

To ensure that the ossicles would behave rigidly, we tested a range of values for

their Young's modulus. A final value of 80 GPa was obtained, beyond which the displacements throughout the model would change by less than 3%. By comparison, in recent finite-element models, the Young's modulus for human ossicles was taken to be 14.1 GPa (Prendergast *et al.*, 1999; Sun *et al.*, 2002) based on Speirs *et al.* (1999), who measured the Young's modulus of human ossicle allografts using axial compression; and 12 GPa (Koike *et al.*, 2002) based on a review by Evans (1973).

The pedicle of the incus was the only part of the ossicles to be represented with volume elements. This decision followed from the work done by Funnell *et al.* (2005), who concluded that the pedicle may not be rigid and may play a major role in the motion between the incus and the stapes. As in their model, a Young's modulus of 5 GPa was assigned to the pedicle based on the measurements of Mente & Lewis (1994). The pedicle had an average thickness of 30 μm and overall dimensions of 70 μm by 140 μm .

The ossicles are linked together by two synovial joints: the incudomalleolar joint and the incudostapedial joint. The incudomalleolar joint was not modelled in this study because it has been observed to be rigid at low frequencies (e.g., Guinan & Peake, 1967; Gundersen *et al.*, 1976). With respect to the incudostapedial joint, Guinan & Peake (1967) and Decraemer *et al.* (1994) reported relative motion between the incus and stapes, but Funnell *et al.* (2005) concluded that this may be attributable mostly to the pedicle, rather than to the incudostapedial joint, a conclusion that was confirmed by Robles *et al.* (2006) in the chinchilla. The incudostapedial joint was therefore not modelled in this study.

In the gerbil, the manubrium of the malleus is tightly connected to the eardrum along its whole length (Oaks, 1967). Therefore, the attachment of the eardrum to the manubrium is represented as a direct connection of the two parts of the model.

3. Ligaments and muscles

According to Rosowski *et al.* (1999), a bony connection exists between the temporal bone of the middle ear and the anterior process of the malleus in gerbils. The histological section in Fig. 2, however, appears to show connective tissue between the temporal bone and the malleus.

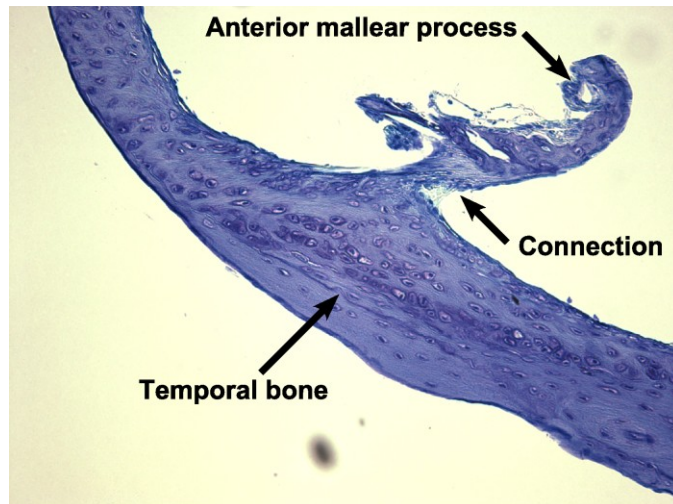


Figure 2: Histological section of the connection between the temporal bone and the anterior process of the malleus, from a set of serial sections. There appears to be connective tissue between the temporal bone and the malleus, corresponding to the anterior mallear ligament.

Fig. 3 presents a section from our MRM data depicting the same region in a different gerbil. The connection between the anterior process of the malleus and the temporal bone is a darker grey than the bone is, which may indicate soft tissue. On the basis of these

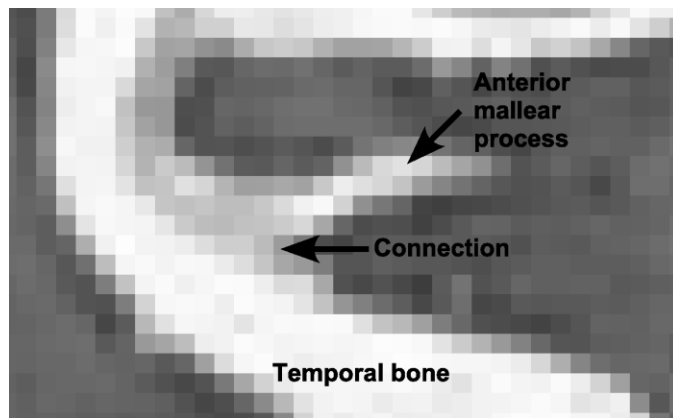


Figure 3: MRM image of the connection between the temporal bone and the anterior process of the malleus. The grey value of the connecting part seems to be different from that of the surrounding bony structures, suggesting the presence of the anterior mallear ligament. Each pixel is 45 μm square.

two images, the connection between the anterior process of the malleus and the temporal bone is modelled as a ligament.

The anterior mallear ligament (AML), the posterior incudal ligament (PIL) and

the stapes annular ligament (SAL) were represented with 288, 457, and 2549 volume elements, respectively. To date, no experimental measurements of the elastic properties of the middle-ear ligaments have been done. Authors have fitted their models to experimental data to determine the Young's modulus of the ligaments (Prendergast *et al.*, 1999; Koike *et al.*, 2002; Sun *et al.*, 2002). In this study, the Young's moduli of the AML and of the PIL were set to 20 MPa as a reasonable value for dense connective tissue, as used in previous models from our lab (Ghosh & Funnell, 1995; Funnell & Decraemer, 1996; Ladak & Funnell, 1996; Funnell *et al.*, 1999, 2000). The AML is connected at one end to the anterior process of the malleus, and is clamped at the other end to represent its attachment to the cavity wall. The AML is about 180 μm in height and about 140 μm in length, and its width varies between about 170 μm and 230 μm . The PIL is composed of two distinct bundles, one medial and the other lateral to the posterior process of the incus. Each bundle is connected to the incus at one end, and is clamped at the other end to represent its attachment to the cavity wall. Each bundle has a somewhat trapezoidal shape. The medial bundle is about 150 μm in height and 100 μm in length, and its width varies between about 70 μm and 160 μm . The lateral bundle is about 160 μm in height and 50 μm in length, and its width varies between about 130 μm and 200 μm .

The Young's modulus of the SAL was set to 10 kPa, in line with vestibular sound-pressure measurements by Lynch *et al.* (1982). This value was also used by Sun *et al.* (2002). The SAL follows the somewhat oval shape of the stapes footplate, with a large diameter of about 1 mm and a short diameter of about 750 μm . The ligament height varies between 50 μm and 170 μm and its thickness varies between 10 μm and 20 μm .

The animal and human experiments that we used for comparison with our model were done either under anaesthesia or post mortem. In such conditions, the muscles are in

a relaxed state. The passive mechanical effects of the two middle-ear muscles (tensor tympani and stapedius) are negligible: Dirckx & Decraemer (2001) found that at very low frequencies the passive muscles do not play a significant role in controlling ossicular motion. The middle-ear muscles were therefore omitted from this model. (This omission might have a significant influence on the simulations presented in Section IV 6 with the stiffnesses of the AML and/or PIL set to zero.)

B. Mesh-resolution convergence

Finite-element results depend in part on how fine a mesh is used to represent the geometry. The mesh resolution is defined in our software by an xy resolution (within slices) and a z resolution (the spacing between slices). As the mesh resolution increases, the computed displacements converge towards the exact solution for the model. However, the number of degrees of freedom also increases and strongly affects computation time. To determine an adequate mesh resolution for our model, we performed a series of runs by varying xy and z resolutions for every structure in the model, with smaller elements used where fine geometrical details need to be modelled. A mesh resolution corresponding to a total of 9208 elements was chosen for the complete final model, the computation time for each run being less than 13 minutes. Beyond that point, the computation time more than doubles but the displacements change by less than 3%.

III. BASIC MODEL RESULTS

Simulation results for the complete gerbil finite-element model – subjected to a uniform low-frequency sound pressure of 1 Pa applied to the eardrum – are presented in

this section. Unless otherwise mentioned, the displacement values given are the magnitudes of the corresponding displacement vectors.

Fig. 4 depicts the displacement pattern of the eardrum. A grey scale is used to represent the displacements, with black for zero displacements and white for the maximum displacement. Lines of constant displacement are also shown for clarity. In this case the displacement values correspond to the vector

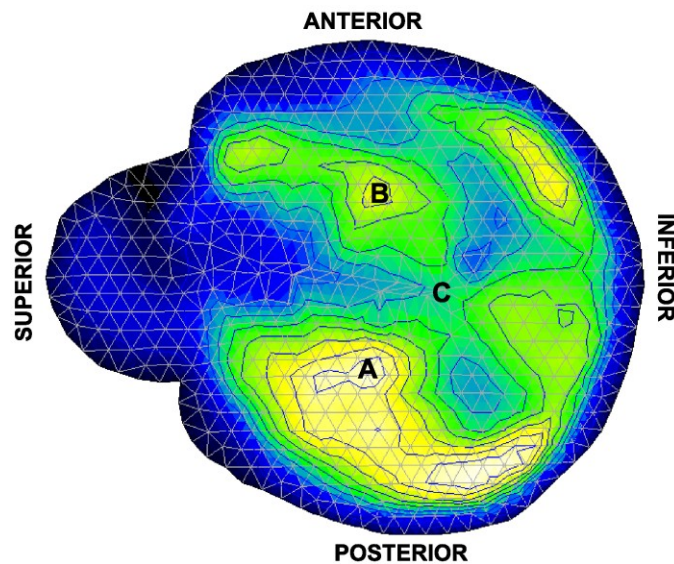


Figure 4: Displacement pattern of the eardrum. A: point of maximum displacement in the posterior region of the eardrum. B: point of maximum displacement in the anterior region of the eardrum. C: point of maximum umbo displacement.

components perpendicular to the plane of the tympanic ring (i.e., the plane of the figure).

The maximum PF displacement is about 65 nm. There are two points of maximum displacement on the PT: one in the posterior region (A) and one in the anterior region (B). The larger of the two maximum displacements is

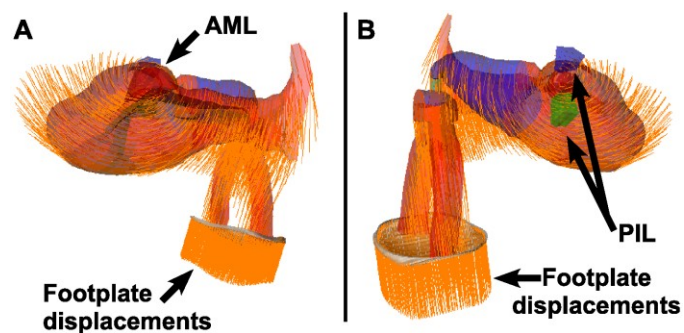


Figure 5: Anterior (A) and posterior (B) views of the ossicles (eardrum and manubrium omitted for clarity). The displacement vectors clearly show the apparent axis of rotation through (A) the anterior malleolar ligament and (B) the posterior incudal ligament.

about 250 nm and lies in the posterior region. The displacement at the umbo (C) is about 105 nm.

Fig. 5 shows the displacement vectors of the ossicles, as viewed along the apparent axis of rotation from the anterior and posterior views. The directions of the vectors clearly show the nature of the rotation about the axis, extending from the posterior incudal ligament to near the anterior malleal ligament.

The footplate displacements are almost completely uniform. The difference between the maximum and minimum footplate displacements is only about 0.24%. This implies a piston-like motion of the stapes, as shown in Fig. 5. The transition from the rotational motion of the incus to the translational motion of the stapes apparently occurs in the flexible pedicle.

IV. SENSITIVITY ANALYSIS

Sensitivity tests attempt to distinguish between the highly influential parameters, whose values must be carefully chosen, and those whose values have little effect on the low-frequency behaviour of the model. The parameters investigated here were (1) the thicknesses of the pars flaccida and pars tensa (T_{pf} and T_{pt} , respectively) and (2) the Young's moduli of the pars flaccida, pars tensa, stapedial annular ligament, anterior malleal ligament, posterior incudal ligament and pedicle (Y_{pf} , Y_{pt} , Y_{sal} , Y_{aml} , Y_{pil} and Y_{ped} , respectively). The effects on the footplate displacements will be examined first, followed by the effects on the eardrum and umbo displacements. These displacements are measures of middle-ear output (footplate) and input (eardrum and umbo), and are commonly studied experimentally. The effects on the umbo-to-stapes ratio and the eardrum-to-umbo ratio will then be presented; these two ratios may be taken as measures of the ossicular lever ratio and of the load transfer between the eardrum and the manubrium, respectively. The effects of the AML and of the PIL on the axis of rotation

of the ossicles will be examined. Finally, the effects of the shape of the eardrum on the overall behaviour of the model will be presented.

1. Footplate displacements

The sensitivity of the model to its eight parameters is shown in Fig. 6. Values for each parameter range from 0.1 to 3 times its nominal value. All curves are monotonic over this range. Overall, as expected, the displacements become smaller as the model becomes stiffer.

Excluding Y_{aml} , when the parameters are decreased by a factor of 10, the footplate displacements increase by 13% (Y_{pil}) to 42% (Y_{ped}). When the same parameters are increased by a factor of 3, footplate displacements decrease by 13% (Y_{pil}) to 56% (T_{pt}). For the Y_{aml} parameter, footplate displacements increase by only 0.6% at a ratio of 0.1, and decrease by only 1.7% at a ratio of 3.

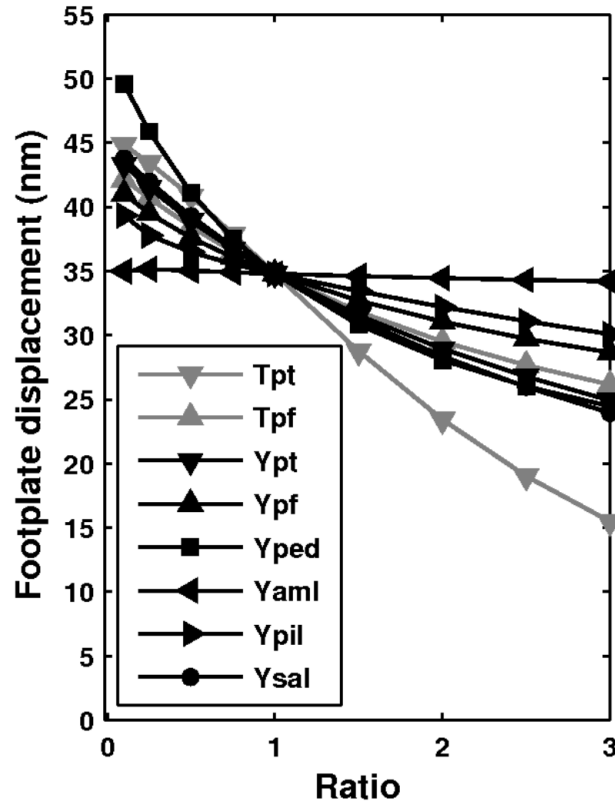


Figure 6: Effect of each parameter on the footplate displacement. The parameters are (1) the thicknesses of the pars flaccida and pars tensa (T_{pf} and T_{pt} , respectively) and (2) the Young's moduli of the pars flaccida, pars tensa, stapedial annular ligament, anterior malleolar ligament, posterior incudal ligament and pedicle (Y_{pf} , Y_{pt} , Y_{sal} , Y_{aml} , Y_{pil} and Y_{ped} , respectively).

The stapes annular ligament (Y_{sal}) has a greater influence on footplate displacements than do the anterior malleolar ligament (Y_{aml}) and the posterior incudal ligament (Y_{pil}). A question arises as to whether Y_{aml} and Y_{pil} may affect the axis of rotation without much affecting the footplate displacement. This will be discussed below.

In a 3-D finite-element model of a cat middle ear, Ghosh & Funnell (1995) represented the ossicles with a fixed axis of rotation and with a simple flexible connection between the incus and the stapes, providing a preliminary implementation of joint flexibility. They varied the incudostapedial joint stiffness from very small to very large values and computed footplate displacements. For very low stiffnesses the footplate displacement decreased because a very soft incudostapedial connection does not transmit force effectively. As the incudostapedial stiffness increased, footplate displacement reached a peak then dropped slightly and stabilized at a constant value.

To look for a similar phenomenon, we varied the stiffness of the pedicle (Y_{ped}) to extreme values in our model. The results are consistent with those of Ghosh & Funnell (1995). The stapes-displacement peak is at 100 MPa in the present model. As the stiffness decreases below 100 MPa, the footplate displacements approach zero because the pedicle becomes too soft to transmit forces well. As the stiffness increases above 100 MPa the footplate displacements again decrease, because the pedicle becomes too stiff to permit the transition from rotational motion to translational motion. The displacements reach a plateau at extremely high stiffnesses because the pedicle is so rigid that any further increase would have a negligible influence on footplate displacements. The peak here is much more prominent than that found by Ghosh & Funnell (1995).

2. Eardrum displacements

The parameters with the greatest effects on PT displacement are the Young's modulus (Y_{pt}) and the thickness (T_{pt}) of the PT itself (Fig. 7). When T_{pt} and Y_{pt} are decreased by a factor of 10, PT displacements increase by a factor of about 37 and 5, respectively. When the same parameters are increased by a factor of 3, PT displacements decrease by about 67% and 42%, respectively. The fact that the thickness has a greater

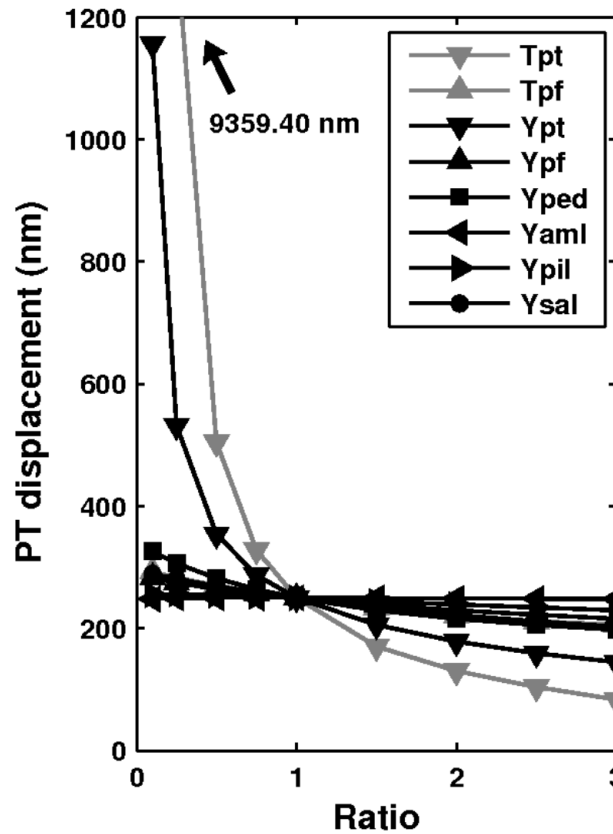


Figure 7: Effect of each parameter on the pars tensa (PT) displacement.

effect than the Young's modulus suggests that the bending stiffness of the eardrum is more important than its in-plane, or membrane, stiffness. This is consistent with classical thin-plate theory, which states that the bending stiffness is proportional to the cube of the thickness while the in-plane stiffness is proportional to the thickness itself.

Four of the remaining six parameters (Y_{ped} , Y_{pf} , T_{pf} and Y_{sal}) have relatively little effect on PT displacements: when they are decreased by a factor of 10, PT displacements increase by about 23%, 12%, 15% and 24%, respectively; when they are increased by a factor of 3, PT displacements decrease by 26%, 16%, 21% and 23%, respectively. The

influence of the last two parameters (Y_{aml} and Y_{pil}) is negligible, with the displacements changing by 2% or less.

3. Umbo displacements

The sensitivity of the umbo to the same eight parameters is shown in Fig. 8. There is relatively little difference between the way in which the various parameters influence the umbo and the way in which they influence the footplate. Compared with Fig. 6, the most noticeable difference is that Y_{aml} has little effect on the umbo at low ratios. When Y_{aml} is decreased by a factor of 10, umbo displacements increase by only about 4%.

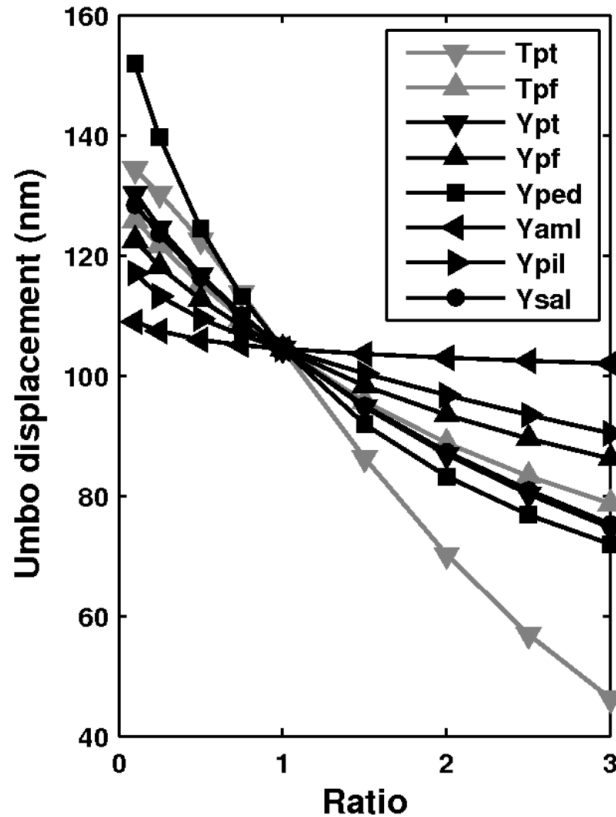


Figure 8: Effect of each parameter on the umbo displacement.

4. Ossicular lever ratio

As a measure of the ossicular lever ratio, we calculated the ratio of the umbo displacement to the stapes displacement (U/S ratio) for each parameter (Fig. 9). The vertical scale is expanded because, as mentioned previously, most of the parameters have approximately the same effects on the umbo and on the footplate.

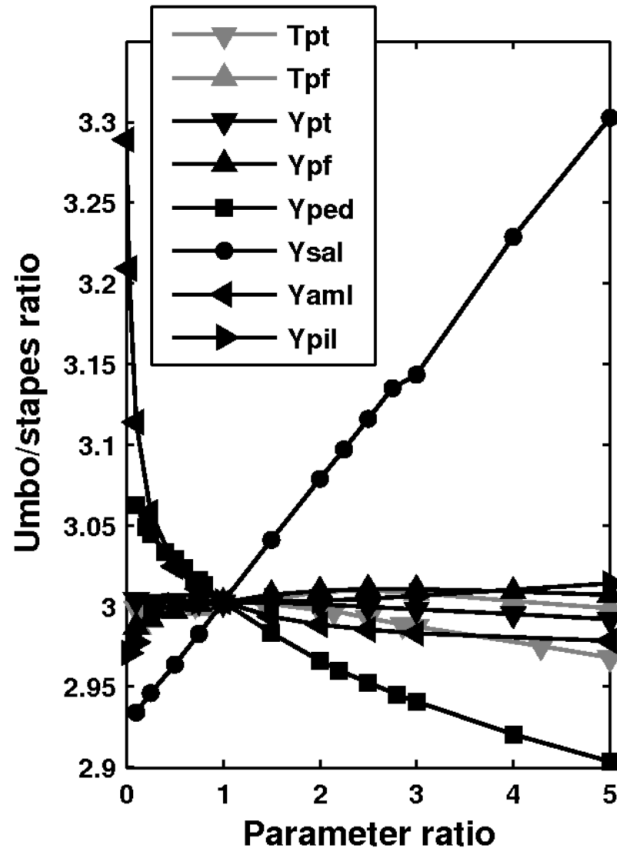


Figure 9: Effect of each parameter on the umbo-to-stapes (U/S) ratio, as a measure of the ossicular lever ratio.

When the stapes annular ligament is stiffened, the stapes footplate displacements decrease more than the umbo displacements do, and the U/S ratio evidently increases. When the anterior malleal ligament becomes less stiff, the malleus is less constrained and lateral motions appear. Lateral motions are not effective in transferring loads across the ossicles, so stapes footplate displacements decrease and the U/S ratio increases.

None of the other parameters had a significant effect on the U/S ratio.

5. Eardrum-manubrium load transfer

To measure the effectiveness of the load transfer from the eardrum to the ossicles, we calculated the ratio of the pars tensa displacement to the umbo displacement (PT/U ratio) for each parameter (Fig. 10), based on the displacement-vector components perpendicular to the plane of the tympanic ring.

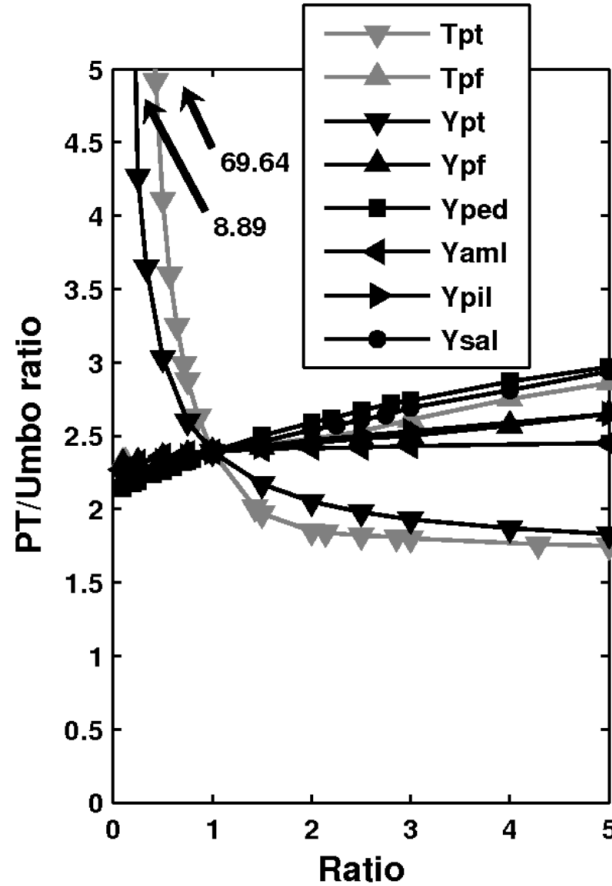


Figure 10: Effect of each parameter on the PT-to-umbo (PT/U) ratio, as a measure of the coupling between the eardrum and the ossicles.

When T_{pt} and Y_{pt} are decreased by a factor of 10, the PT/U ratio increases by factors of about 28 and 2, respectively. When T_{pt} and Y_{pt} are increased by a factor of 5, the PT/U ratio decreases by about 27% and 23%, respectively. For the other six parameters, the changes in the PT/U ratio are smaller and in the opposite direction. As the eardrum becomes less stiff, it cannot displace the ossicles and the PT/U ratio increases. On the other hand, as the ossicular system becomes less stiff, the umbo displacements increase and the PT/U ratio decreases.

6. Axis of rotation

In an attempt to understand how the apparent axis of rotation is influenced by the anterior malleolar ligament (AML) and the posterior incudal ligament (PIL), we ran simulations on the model for six different cases (see Fig. 11):

- A: The AML and the PIL are kept intact.
- B: The Young's modulus of both the AML and the PIL are set to zero.
- C: Only the Young's modulus of the AML is set to zero.
- D: Only the Young's modulus of the PIL is set to zero.
- E: Only the Young's modulus of the AML is increased by a factor of 10.
- F: Only the Young's modulus of the PIL is increased by a factor of 10.

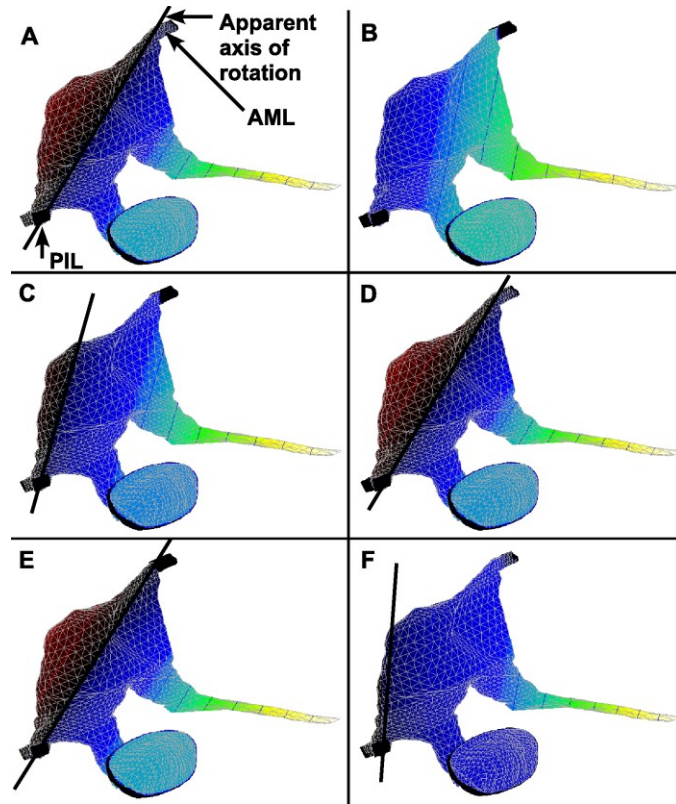


Figure 11: Effect of removing and stiffening the anterior malleolar ligament (AML) and the posterior incudal ligament (PIL) on the apparent axis of rotation. **A:** the AML and the PIL are kept intact. **B:** the Young's modulus of both the AML and the PIL are set to zero. **C:** only the Young's modulus of the AML is set to zero. **D:** only the Young's modulus of the PIL is set to zero. **E:** only the Young's modulus of the AML is increased by a factor of 10. **F:** only the Young's modulus of the PIL is increased by a factor of 10.

In case A, we can see (as described previously) that the apparent axis of rotation

passes through the AML and the PIL.

When both the AML and the PIL have a Young's modulus of zero (case B), the axis of rotation is shifted to the left and completely outside the figure. The parallel contour lines indicate the direction of the axis of rotation. Footplate and umbo displacements increase by about 46% and 29%, respectively. The umbo-to-stapes (U/S) ratio decreases by about 12%.

When the Young's modulus of the AML is set to zero (case C), the anterior end of the axis of rotation is shifted to the left of the AML, and the axis still passes through the PIL. Footplate displacements decrease by only about 3%, and umbo displacements increase by about 7%. The U/S ratio is increased by about 10%.

In case D, when the Young's modulus of the PIL is set to zero, the posterior end of the axis of rotation is shifted slightly to the right of the PIL (clearly by a lesser amount than in case C), and the axis still passes through the AML. Footplate and umbo displacements both increase by about 18%. The U/S ratio is almost unchanged.

When the Young's modulus of the AML is stiffened (case E), the axis of rotation is shifted slightly to the right at both ends. Footplate and umbo displacements both decrease by about 65%. The U/S ratio decreases by about 1.5%.

When the PIL is stiffened (case F), the anterior end of the axis of rotation is shifted considerably to the left of the AML. Footplate and umbo displacements are decreased to 0.7% and 1.3% of their initial values, respectively, and the U/S ratio is increased by about a factor of 2.

In summary:

- When the AML is cut, there is a large axis change but a relatively small change in the ossicular ratio (about 10%).

- When the PIL is cut, there is a very small axis change and no change in the ossicular ratio.
- When the AML is stiffened, there is practically no change in the axis or in the ossicular ratio.
- When the PIL is stiffened, there is a large axis change but only a moderate change in the ossicular ratio (by a factor of 2).

7. Eardrum shape

Funnell & Laszlo (1978) developed a finite-element model of the cat eardrum with a rudimentary middle-ear representation. The shape of the eardrum was defined by a normalized radius-of-curvature parameter. They varied the depth of the cone of the eardrum and the degree of curvature and

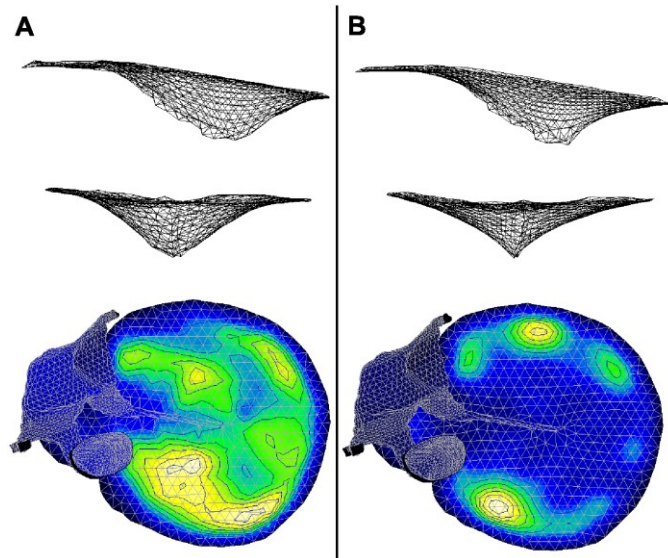


Fig. 12: Effect of changing the shape of the eardrum. A: eardrum in side and front views, before relaxing the shape. B: eardrum in side and front views after relaxing the shape.

showed that the shape of the eardrum has a significant influence on middle-ear mechanics. The effects of eardrum shape were also demonstrated in models by Funnell & Decraemer (1996). In this section, we provide preliminary results on the effects of changing the eardrum shape of our model by presenting just one additional eardrum shape. The new shape was obtained by iterative Laplacian smoothing: each node on the

eardrum is moved in turn to the position which is the average of the positions of all the nodes to which it is connected. The same process is repeated until none of the nodes moves more than some threshold amount.

Fig. 12 shows the eardrum based on the MRM data (A) and the newly shaped eardrum (B), in side and front views, and their displacement patterns. The modified eardrum is steeper near the periphery and near the manubrium, and has a more uniform curvature. The displacement pattern in A is the same as that in Fig. 4. In B, two areas of maximum displacement are again seen, but they are further away from the manubrium and closer to the annular ring than they are in A, and they are more localized. The maximum displacement in B appears in the posterior region, as it does in A. Maximum eardrum displacement increased from about 250 nm (A) to about 334 nm (B). Umbo displacement, however, decreased from about 105 nm (A) to about 40 nm (B), and stapes displacement decreased from about 35 nm (A) to about 13 nm (B). The ossicular lever ratio (U/S ratio) is thus almost identical in A and B, but the PT/U ratio increased from 2.4 (A) to 8.4 (B), indicating that the modified eardrum shape is less effective in driving the ossicular chain.

V. COMPARISON WITH EXPERIMENTAL MEASUREMENTS

To validate our model, we compared its behaviour with experimental data. The model has no inertial or damping terms and is therefore applicable to low acoustic frequencies.

1. Eardrum measurements

Von Unge *et al.* (1993) measured the displacement patterns of the gerbil eardrum

under quasi-static pressures with a real-time moiré interferometer. Two points of maximum displacement were reported: one in the anterior part, slightly superior to the umbo, and one in the posterior part, somewhat more superiorly. The larger of the two was in the posterior region. These findings are consistent with the results from our eardrum model (Fig. 4) with respect to the positions of the points of maximum displacement. In terms of the displacements themselves, our model values (for low acoustic frequencies) are expected differ from the experimental results because of viscoelastic effects in the quasi-static measurements, and because the experimental pressures were very high and the measured displacements were thus non-linear.

2. Ossicular measurements

Although a number of studies have produced experimental measurements on gerbil middle ears, few have included responses below 1 kHz. Ravicz & Rosowski (1997), Overstreet & Ruggero (2002) and Overstreet *et al.* (2003) dealt exclusively with high-frequency responses. Rosowski *et al.* (1999), Olson & Cooper (2000) and Ravicz & Rosowski (2004) looked at both low and high frequencies.

Rosowski *et al.* (1999) and Ravicz & Rosowski (2004) used a probe-tube microphone and a laser Doppler vibrometer to measure stapes displacements at the posterior crus. The laser beam was focused at an angle of between 30 and 45 degrees relative to the direction of piston-like stapes translation. A cosine correction was used to adjust all laser measurements to a value consistent with the supposed direction of translation. Olson & Cooper (2000) used an interferometer to measure the stapes displacements at specified points on the footplate.

Only Rosowski *et al.* (1999) measured displacements at, or at least near, the

umbo. To date, no measurements of gerbil eardrum displacements have been made.

The experimentally measured stapes velocities increase linearly with frequency (i.e., the displacements are constant) up to about 1 kHz, indicating that the system is

Displacements (nm)	Model	Rosowski et al. (1999)	Olson & Cooper (2000)	Ravicz & Rosowski (2004)
Pars tensa	250	-	-	-
Umbo	104.5	183.8	-	-
Footplate	34.8	52.5	47.7	35

Table 1: Summary of gerbil middle-ear experiments.

stiffness-dominated over that frequency range. The behaviour becomes more complex beyond 1 kHz, as inertia and damping become significant. Only the low-frequency results will be used for the comparison with our finite-element model. We averaged the values from Rosowski *et al.* (1999), Olson & Cooper (2000) and Ravicz & Rosowski (2004) across a frequency range of 100 Hz to 1 kHz. The data from Olson & Cooper (2000) were taken from Ravicz & Rosowski (2004). For comparison with our displacement results, we converted the reported stapes velocities to displacements by dividing by the frequency. These results are compared with our model results in Table 1.

Our umbo displacement differs from that of Rosowski *et al.* (1999) by about 43%. Our footplate displacement differs from those of Rosowski *et al.* (1999) and Olson & Cooper (2000) by approximately 33% and 27%, respectively, and is almost identical to the value obtained by Ravicz & Rosowski (2004).

The ratio of umbo displacement to stapes footplate displacement (U/S) gives an indication of the ossicular lever ratio, which is one of the factors often used to define the energy-transfer mechanism of the middle ear. Rosowski *et al.* (1999) reported an ossicular lever ratio of about 3.5. In our model the ratio is 3.0. Keeping in mind the variability of the experimental data, this agrees quite well with their value. The value of

3.5 is outside the range of values seen in Fig. 9 for different model parameters. As noted above, none of the parameters have a strong effect on U/S, but varying the geometry of the ossicles and ligaments presumably would.

3. Ligament measurements

The apparent axis of rotation observed in our model is similar to the classical description given in the literature for low frequencies, namely, passing from the anterior malleolar ligament (AML) to the posterior incudal ligament (PIL).

Nakajima *et al.* (2004) determined the effects both of stiffening and of removing the AML and the PIL in fresh human ossicles. Sound-induced umbo and stapes velocities were measured by laser vibrometry. Stiffening of the AML resulted in a decrease of umbo and stapes displacements by a factor of 2 or less. In our model, the umbo and stapes displacements decreased by 65%. No experimental studies have included the effects of stiffening the PIL.

Experimental removal of the AML resulted in an increase in umbo displacements of less than 60% and a change in footplate displacements of less than 30%. Removal of the PIL resulted in an increase in umbo displacements of less than 40% and a change in footplate displacements of less than 15%. In our model, when the stiffness of the AML was set to zero, the umbo displacements increased by only 7% and the stapes footplate displacements decreased by only 3%. When the stiffness of the PIL was set to zero, the umbo and stapes displacements both increased by 18%. If the middle-ear muscles were added to the model, these changes would presumably be smaller.

Nakajima *et al.* (2004) concluded that removal of either the AML or the PIL affects ossicular motion only minimally at low frequencies. Large and complex changes

were reported, however, when both the AML and the PIL were removed. These results are qualitatively consistent with our findings.

VI. DISCUSSION

A finite-element model of the gerbil middle ear was developed. The behaviour of this model in response to a low-frequency sound pressure of 1 Pa was analyzed. Sensitivity tests were performed to evaluate the significance of the different parameters in the finite-element model. To validate the model, we compared our results with experimental data from the literature.

The Young's modulus and the thickness of the PT had the greatest effect on PT displacements and, along with the Young's moduli of the pedicle and the stapedial annular ligament (SAL), on umbo and stapes displacements. The Young's moduli of the PIL and the AML had the least effect on the model. The ossicular lever ratio (umbo-to-stapes ratio) was relatively insensitive to all parameters. The coupling between the eardrum and the manubrium (PT-to-umbo ratio) was found to be highly affected by the pars-tensa parameters, and to a lesser extent by the thickness of the PF and by the Young's moduli of the pedicle and the SAL. Finally, the shape of the eardrum was shown to have an effect on the displacements of the middle-ear components, and on the displacement profile of the eardrum itself.

Overall, our finite-element model demonstrates good agreement with experimental data. The displacement pattern of the PT in our model is similar in shape to profiles measured experimentally (von Unge *et al.*, 1993). The umbo and stapes displacements, as well as the ossicular displacement ratio, compare satisfactorily with low-frequency measurements from Rosowski *et al.* (1999), Olson & Cooper (2000) and

Ravicz & Rosowski (2004). The ossicular axis of rotation extended from the anterior malleolar ligament (AML) to the posterior incudal ligament (PIL), corresponding to the classical description, and the motion of the stapes is piston-like, in agreement with the low-frequency observations of Decraemer *et al.* (2005).

The axis of rotation was influenced by the AML when it was cut, by the PIL when it was stiffened, and by both together when they were cut. The corresponding changes of ossicular displacements are comparable to those of Nakajima *et al.* (2004).

The umbo and stapes displacements decreased by 65% when the Young's modulus of the AML was increased by a factor of 10. This is comparable to the findings in human models by Abou-Khalil *et al.* (2001) and Huber *et al.* (2003).

The present model is a step towards detailed quantitative models that can be validated against the considerable body of experimental data on the gerbil middle ear, and in turn can help explain those data.

Several enhancements should be undertaken to improve the model. (1) Inertial and damping properties should be included in the model to permit simulations at higher frequencies. This would allow comparison with the non-piston-like stapes motion observed by Decraemer *et al.* (2005). (2) The study should be extended to non-linear analysis. The large (non-linear) displacements could be compared with recent moiré data from Decraemer's lab (Decraemer *et al.*, 2003; Dirckx & Decraemer, 2003). (3) In our study, the periphery of the eardrum was assumed to be fixed. If an explicit representation of the fibrocartilaginous ring (including the smooth-muscle cells) were included in the model, the behaviour of the model could be compared with the results of studies in which the physiological effects of the smooth muscle were investigated through the administration of drugs known to relax or contract smooth muscle (Yang & Henson,

2002). (4) The study of the effects of different eardrum shapes should be extended. (5) A more thorough representation of the pedicle, the incudomalleolar and incudostapedial joints, the stapedius and tensor tympani muscles, and the ligament/bone connections would serve to improve our understanding of ossicular motion. One specific area to be clarified is whether the connection of the anterior process of the malleus to the wall of the middle-ear air cavity is bony, as observed by Rosowski *et al.* (1999), or ligamentous as suggested by our histological and MRM data. (6) Orthotropic material properties for the eardrum should be investigated and the resulting behaviour compared with the isotropic case.

Displacement measurements on the gerbil eardrum need to be made in order to validate this model properly, and measurements of displacement vectors at multiple locations on the ossicles would also be helpful.

ACKNOWLEDGEMENTS

This work was supported by the Canadian Institutes of Health Research and the Natural Sciences and Engineering Research Council (Canada). We thank M.M. Henson and O.W. Henson, Jr., (UNC-Chapel Hill) and the Center for In Vivo Microscopy (Duke University) for the data used for the MRM-based model. We also thank W.F. Decraemer (University of Antwerp, Belgium) for the X-ray micro-CT and moiré data, and M. von Unge (Karolinska Institute, Sweden) for the histological serial sections. Finally, we thank J. Lauzière for editing the manuscript.

REFERENCES

Abou-Khalil S., Funnell W.R.J., Zeitouni A.G., Schloss M.D. & Rappaport J. (2001):

- “Finite-element modeling of anterior malleolar ligament fixation.” *Eastern Section Meeting, Triological Soc., Toronto.*
- Beer H. J., Bornitz M., Hardtke H.J., Schmidt R., Hofmann G., Vogel U., Zahnert T. & Huttenbrink K.B. (1999): “Modelling of components of the human middle ear and simulation of their dynamic behavior.” *Audiol. NeuroOtol.* 4: 156–162.
- Békésy G.v. (1949): “The structure of the middle ear and the hearing of one’s own voice by bone conduction.” *J. Acoust. Soc. Am.* 21: 217-232.
- Bornitz M., Zahnert T., Hardtke H.J. & Huttenbrink K.B. (1999) “Identification of parameters for the middle ear model.” *Audiol. NeuroOtol.* 4: 163–169.
- Decraemer W.F., Maes M.A. & Vanhuysse V.J. (1980): “An elastic stress-strain relation for soft biological tissues based on a structural model.” *J. Biomech.*, 13: 463-468.
- Decraemer W.F., Gea S.L.R. & Dirckx J.J.J. (2003): “Three-dimensional displacement of the gerbil ossicular chain under static pressure changes.” *26th ARO MidWinter Mtg.*
- Decraemer W.F., Khanna S.M., De la Rochefoucauld O., Dong W. and Olson E.S. (2005): “Is the scala vestibuli pressure influenced by non-piston like stapes motion components? An experimental approach.” *Auditory mechanisms: processes and models*, Proc. Ninth International Mechanics of Hearing Workshop, Portland (OR).
- Dirckx JJJ & Decraemer WF (1989): “Phase shift moiré apparatus for automatic 3-D surface measurement.” *Rev. Sci. Instr.* 60: 3698-3701.
- Dirckx JJJ & Decraemer WF (1990): “Automatic calibration method for phase shift shadow moiré interferometry.” *Appl. Opt.* 29: 1474-1476.
- Dirckx J.J.J. & Decraemer W.F. (2001): “Effect of middle ear components on eardrum

- quasi-static deformation.” *Hearing Res.* 157: 124-137.
- Dirckx J.J.J. & Decraemer W.F. (2003): “Pressure Induced Eardrum Deformation at Progressive Stages of Middle Ear Dissection.” *26th ARO MidWinter Mtg.*
- Evans F.G. (1973): *Mechanical properties of bone*. Thomas, Springfield, IL, p. 35.
- Fay J., Puria S., Decraemer W.F. & Steele C. (2005): “Three approaches for estimating the elastic modulus of the tympanic membrane.” *J. Biomech.* 38: 1807-1815.
- Funnell W.R.J. & Laszlo C.A. (1978): “Modeling of the cat eardrum as a thin shell using the finite-element method.” *J. Acoust. Soc. Am.* 63: 1461–1467.
- Funnell W.R.J., Decraemer W.F. & Khanna S.M. (1987): “On the damped frequency response of a finite-element model of the cat eardrum.” *J. Acoust. Soc. Am.* 81: 1851–1859.
- Funnell W.R.J., Khanna S.M. & Decraemer W.F. (1992): “On the degree of rigidity of the manubrium in a finite-element model of the cat eardrum.” *J. Acoust. Soc. Am.* 91: 2082-2090.
- Funnell W.R.J. & Decraemer W.F. (1996): “Finite-element modelling of the cat middle ear with elastically suspended malleus and incus.” *19th ARO MidWinter Meeting.*
- Funnell W.R.J., Decraemer W.F., Von Unge M. & Dirckx J.J.J. (1999): “Finite-element modelling of the gerbil eardrum and middle ear.” *22rd ARO MidWinter Meeting.*
- Funnell W.R.J., Decraemer W.F., Von Unge M. & Dirckx J.J.J. (2000): “Finite-element modelling of the gerbil eardrum and middle ear.” *23rd ARO MidWinter Meeting.*
- Funnell W.R.J., Siah T.H., McKee M.D., Daniel S.J. & Decraemer W.F. (2005): “On the coupling between the incus and the stapes in the cat.” *J. Acoust. Res. Otol.* 6: 9-18.
- Ghosh S.S. & Funnell W.R.J. (1995): “On the effects of incudostapedial joint flexibility

- in a finite-element model of the cat middle ear.” *Proc. IEEE-EMBS 17th Annual Conference and 21st Can. Med. & Biol. Eng. Conf., Montreal*, 1437-1438.
- Guinan Jr. J.J. & Peake W.T. (1967): “Middle-ear characteristics of anesthetized cats.” *J. Acoust. Soc. Am.* 41: 1237-61.
- Gundersen T. (1976): “Holographic vibration analysis of the ossicular chain.” *Acta Otolaryngol.* 82: 16-25.
- Huber A., Koike T., Wada H., Nandapalan V. & Fisch U. (2003): “Fixation of the anterior malleolar ligament: diagnosis and consequences for hearing results in stapes surgery.” *Ann. Otol. Rhinol. Laryngol.* 112: 348–355.
- Koike T., Wada H. & Kobayashi T. (2002): “Modeling of the human middle ear using the finite-element method.” *J. Acoust. Soc. Am.* 111: 1306-1317.
- Kuypers L.C., Dirckx J.J.J. Decraemer W.F. & Timmermans J.-P. (2005): “Thickness of the gerbil tympanic membrane measured with confocal microscopy.” *Hearing Res.* 209: 42-52.
- Ladak H.M. & Funnell W.R.J. (1996): “Finite-element modeling of the normal and surgically repaired cat middle ear.” *J. Acoust. Soc. Am.* 100: 933–944.
- Lynch T.J., Nedzelnitsky V. & Peake W.T. (1982): “Input impedance of the cochlea in cat.” *J. Acoust. Soc. Am.* 72: 108-130.
- Mente P.L. & Lewis J.L. (1994): “Elastic modulus of calcified cartilage is an order of magnitude less than that of subchondral bone.” *J. Orthopaedic Res.* 12: 637–647.
- Nakajima H.H., Peake W.T., Rosowski J.J. & Merchant S.N. (2004): “Ossicular ligaments and the axis of rotation.” *27th ARO MidWinter Meeting*.
- Oaks E (1967): *Structure and function of inflated middle ears of rodents*. Ph. D. thesis (Yale University, New Haven)

- Olson E. & Cooper N. (2000): "Stapes motion and scala vestibuli pressure in gerbil." *23rd ARO MidWinter Meeting*.
- Overstreet E.H., Richter C.P., Temchin A.N., Cheatham M.A. & Ruggero M.A. (2003): "High-frequency sensitivity of the mature gerbil cochlea and its development." *Audiol. NeuroOtol.* 8: 19-27.
- Prendergast P.J., Ferris P., Rice H.J. & Blayney A.W. (1999): "Vibroacoustic modelling of the outer and middle ear using the finite-element method." *Audiol. NeuroOtol.* 4: 185–191.
- Qi L., Mikhael C.S. & Funnell W.R.J. (2004): Application of the Taguchi method to sensitivity analysis of a middle-ear finite-element model. *Proc. 28th Ann. Conf. Can. Med. Biol. Eng. Soc.*, 153-156.
- Ravicz M.E. & Rosowski J.J. (2004): "High-frequency sound transmission through the gerbil middle ear." *27th ARO MidWinter Meeting*.
- Robles L., Temchin A., Fan Y.-H., Cai H. & Ruggero M. (2006): "Vibrations of the Stapes and the Long and Lenticular Processes of the Incus in the Chinchilla Middle Ear." *29th ARO MidWinter Meeting*.
- Rosowski J.J., Ravicz M.E., Teoh S.W. & Flandermeyer D. (1999): "Measurements of middle-ear function in the Mongolian gerbil, a specialized mammalian ear." *Audiol. NeuroOtol.* 4(3-4): 129-136.
- Speirs A.D., Hotz M.A., Oxland T.R., Hausler R. & Nolte L.-P. (1999): "Biomechanical properties of sterilized human auditory ossicles." *J. Biomech.* 32: 485-491.
- Sun Q., Gan R.Z., Chang K.H. & Dormer K.J. (2002): "Computer-integrated finite-element modeling of human middle ear." *Biomechan. Model. Mechanobiol.* 1: 109-122.

- Van Wijhe R.G., Funnell W.R.J., Henson O.W. Jr. & Henson M.M. (2000):
“Development of a finite-element model of the middle ear of the moustached
bat.” *Proc. 26th Ann. Conf. Can. Med. Biol. Eng. Soc.*, 20-21
- Von Unge M., Decraemer W.F., Bagger-Sjoback D. & Dirckx J.J.J. (1993):
“Displacement of the gerbil tympanic membrane under static pressure variations
measured with a real-time differential moiré interferometer.” *Hearing Res.* 70:
229-242.
- Wada H., Metoki T. & Kobayashi T. (1992): “Analysis of dynamic behavior of human
middle ear using a finite-element method.” *J. Acoust. Soc. Am.* 92 : 3157–3168.
- Yang X. & Henson O.W. Jr. (2002): “Smooth muscle in the annulus fibrosus of the
tympanic membrane: physiological effects on sound transmission in the gerbil.”
Hearing Res. 164: 105-114.